Chapter 2
Ultra-Broadband Optical Parametric Amplifiers

Giulio Cerullo and Daniele Brida

2.1 Introduction

Many modern studies of light-matter interaction require optical pulses with short durations as well as broad frequency tuneability. Both properties are of utmost importance for time-resolved optical spectroscopy and high-field physics. In femtosecond pump-probe spectroscopy, the system under study (atom, molecule or solid) is resonantly excited by a "pump" pulse and its subsequent evolution is monitored by measuring the pump-induced transmission change of a delayed "probe" pulse [1]. To be able to probe elementary photophysical and photochemical relaxation processes, it is necessary to push the temporal resolution towards the limit set by the oscillation period of the carrier wave. The need to excite a system on resonance and probe optical transitions occurring at different photon energies requires broad frequency tuneability of both pump and probe pulses [2]. On the other hand, by focusing high-intensity ultrashort pulses in a noble gas jet, it is possible to produce coherent bursts of XUV radiation by the so-called High Harmonic Generation (HHG) process [3] (See Chap. 3 by Marangos et al. and Chap. 7 by Mathias et al.). Also for the HHG process, wavelength tuneability of the driver pulses is important, since it influences both the frequency extension and the phase-matching conditions of the XUV pulses. In view of the above mentioned applications, the generation of tuneable few-optical-cycle light pulses is one of the major challenges of ultrafast optics [4].

Nowadays, several reliable sources of femtosecond pulses exist, based for example on Ti:sapphire or Ytterbium technologies; however they emit only at fixed frequencies. Despite this limitation, the very high peak power of these sources enables exploiting the second order nonlinear optical effect known as Optical

G. Cerullo (✉) • D. Brida
Dipartimento di Fisica, Politecnico di Milano, Piazza L. da Vinci 32, 20133 Milan, Italy
e-mail: giulio.cerullo@fisi.polimi.it

R. Thomson et al. (eds.), *Ultrafast Nonlinear Optics*, Scottish Graduate Series, DOI 10.1007/978-3-319-00017-6_2,

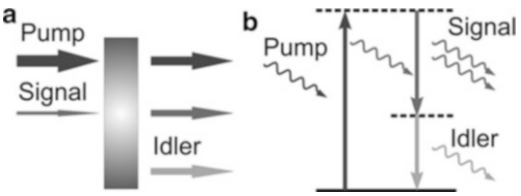

Fig. 2.1 (**a**) Optical Parametric Amplification in a non-centrosymmetric nonlinear crystal (**b**) corpuscular interpretation of the OPA process

Parametric Amplification (OPA) [5, 6] to extend their tuning range. The principle of OPA is quite simple (Fig. 2.1a): in a suitable nonlinear crystal, energy is transferred from a high frequency and high intensity beam (the pump beam, at frequency ω_3) to a lower frequency, lower intensity beam (the signal beam, at frequency ω_1) which is thus amplified; in addition a third beam (the idler beam, at frequency ω_2) is generated. The OPA process can be given a simple corpuscular interpretation (see Fig. 2.1b): a photon at frequency ω_3 is absorbed by a virtual level of the material and a photon at frequency ω_1 stimulates the emission of two photons at frequencies ω_1 and ω_2. In this interaction energy conservation:

$$\hbar\omega_3 = \hbar\omega_1 + \hbar\omega_2 \tag{2.1}$$

is fulfilled. The signal frequency to be amplified can vary in principle from $\omega_3/2$ (the so-called *degeneracy condition*, with $\omega_1 = \omega_2$) to ω_3, and correspondingly the idler varies from $\omega_3/2$ to 0 (as a matter of the fact the lowest frequency is limited by absorption of the nonlinear crystal).

In summary, the OPA process transfers energy from a high-power, fixed frequency pump beam to a low-power, variable frequency signal beam, generating an idler beam to satisfy energy conservation. The OPA process thus provides an optical amplifier with continuously variable centre frequency and represents an easy way of tuning over a broad range the frequency of an otherwise fixed femtosecond laser system. On the other hand, if suitably designed, an OPA can have a very broad amplification bandwidth and thus efficiently transfer energy from a narrowband pump pulse to a broadband signal pulse; it can therefore be used to dramatically shorten, by more than an order of magnitude, the duration of the pump pulse. The concept of broadband OPA is very flexible and can be applied to produce few-optical-cycle pulses over a very wide frequency range, provided that a broadband yet weak seed is available and the proper phase-matching conditions are identified.

This chapter reviews the principles of ultrashort pulse OPAs, focusing in particular on the generation of few-optical-cycle pulses. It is organized as follows: Section 2.2 discusses the propagation of an ultrashort pulse in a nonlinear medium; Sect. 2.3 reviews the theory of parametric amplification for the case of monochromatic waves; Sect. 2.4 extends it to the case of ultrashort pulses; Sect. 2.5 discusses the architecture of ultrafast OPAs and gives a relevant example; Sect. 2.6 reviews ultra-broadband OPAs; Sect. 2.7 explains how OPAs can be used to stabilize the carrier-envelope phase of ultrashort pulses; finally, Sect. 2.8 introduces the concept of optical parametric chirped pulse amplification, the most promising approach for energy scaling of ultrashort pulses.

2.2 Ultrashort Pulse Propagation in a Nonlinear Medium

In this section we briefly derive the equation for the propagation of an ultrashort pulse in a dispersive nonlinear medium, that will be used in the remainder of the chapter [6–8]. We start from Maxwell's propagation equation for the electric field E of a scalar plane wave:

$$\frac{\partial^2 E}{\partial z^2} - \frac{1}{c_0^2}\frac{\partial^2 E}{\partial t^2} = \mu_0 \frac{\partial^2 P}{\partial t^2} \tag{2.2}$$

where c_0 is the speed of light in vacuum and P is the polarisation describing the medium response. We write the electric field as:

$$E(z,t) = \mathrm{Re}\{A(z,t)\exp[i(\omega_0 t - k_0 z)]\} = \frac{1}{2}\{A(z,t)\exp[i(\omega_0 t - k_0 z)] + c.c.\} \tag{2.3}$$

where $A(z,t)$ is the *complex field envelope*. In the following we will for simplicity drop the notation $\mathrm{Re}\{\ldots\}$. The polarisation can be decomposed in the sum of a linear (P_L) and a non-linear (P_{NL}) component:

$$P(z,t) = P_L(z,t) + P_{NL}(z,t) \tag{2.4}$$

Let us initially consider only the linear component of the polarisation:

$$P_L(z,t) = p_L(z,t)\exp[i(\omega_0 t - k_0 z)] \tag{2.5}$$

and solve the equation:

$$\frac{\partial^2 E}{\partial z^2} - \frac{1}{c_0^2}\frac{\partial^2 E}{\partial t^2} = \mu_0 \frac{\partial^2 P_L}{\partial t^2} \tag{2.6}$$

Equation (2.6) is more easily solved in the frequency domain, by introducing the Fourier transforms:

$$\tilde{E}(z,\omega) = \tilde{A}(z,\omega-\omega_0)\exp(-ik_0 z) \tag{2.7a}$$

$$\tilde{P}_L(z,\omega) = \tilde{p}_L(z,\omega-\omega_0)\exp(-ik_0 z) \tag{2.7b}$$

and becomes:

$$\frac{\partial^2 \tilde{E}}{\partial z^2} + \frac{\omega^2}{c_0^2}\tilde{E} = -\mu_0\omega^2\tilde{P}_L \tag{2.8}$$

which, with the help of (2.7), can be rewritten as:

$$\frac{\partial^2 \tilde{A}}{\partial z^2} - 2ik_0 \frac{\partial \tilde{A}}{\partial z} - k_0^2 \tilde{A} + \frac{\omega^2}{c_0^2} \tilde{A} = -\mu_0 \omega^2 \tilde{p}_L \tag{2.9}$$

We now make the Slowly Varying Envelope Approximation (SVEA), which consists in assuming that $\frac{\partial^2 \tilde{A}}{\partial z^2} \ll k_0 \frac{\partial \tilde{A}}{\partial z}$; this corresponds to neglecting variations of the envelope over propagation lengths of the order of the wavelength. With this assumption we obtain:

$$-2ik_0 \frac{\partial \tilde{A}}{\partial z} - k_0^2 \tilde{A} + \frac{\omega^2}{c_0^2} \tilde{A} = -\mu_0 \omega^2 \tilde{p}_L \tag{2.10}$$

From the definition of refractive index $n(\omega)$, we can write:

$$\tilde{p}_L(\omega) = \varepsilon_0 \left[n^2(\omega) - 1 \right] \tilde{A}(\omega) \tag{2.11}$$

and obtain:

$$2ik_0 \frac{\partial \tilde{A}}{\partial z} = \left[k^2(\omega) - k_0^2 \right] \tilde{A} \tag{2.12}$$

with $k(\omega) = \frac{\omega}{c_0} n(\omega)$. In a dispersive medium, the refractive index is a function of frequency, and the wavenumber thus becomes a nonlinear function of ω. We can further approximate:

$$k^2(\omega) - k_0^2 \cong 2k_0 \left[k(\omega) - k_0 \right] \tag{2.13}$$

We now perform a Taylor expansion of $k(\omega)$ around ω_0:

$$k(\omega) = k_0 + k_0' (\omega - \omega_0) + \frac{1}{2} k_0'' (\omega - \omega_0)^2 + \ldots \tag{2.14}$$

where $k_0' = \left(\frac{dk}{d\omega} \right)_{\omega_0} = \frac{1}{v_{g0}}$, v_{g0} being the group velocity of the carrier frequency and $k_0'' = \left(\frac{d^2 k}{d\omega^2} \right)_{\omega_0}$ the Group Velocity Dispersion (GVD). Usually an expansion up to the second order is sufficient, with the third order required only for very broad pulse bandwidths. Equation (2.12) then becomes:

$$i \frac{\partial \tilde{A}(\omega - \omega_0)}{\partial z} \cong \frac{1}{v_{g0}} (\omega - \omega_0) \tilde{A} + \frac{1}{2} k_0'' (\omega - \omega_0)^2 \tilde{A} \tag{2.15}$$

We can transform (2.15) back to the time domain, obtaining:

$$\frac{\partial A\,(z,t)}{\partial z}+\frac{1}{v_{g0}}\frac{\partial A}{\partial t}-\frac{i}{2}k''_0\frac{\partial^2 A}{\partial t^2}=0 \tag{2.16}$$

Equation (2.16) describes the linear propagation of a pulse in a dispersive medium. We now introduce the nonlinear polarisation, which can be written as:

$$P_{NL}\,(z,t)=p_{NL}\,(z,t)\exp\left[i\,\left(\omega_0 t-k_p z\right)\right] \tag{2.17}$$

We have emphasized that the wavenumber k_p of the nonlinear polarisation at ω_0 is different from that of the electric field. Matching of the wave-vectors $k_p = k_0$ (phase matching) is the key for an efficient nonlinear interaction. If we make the approximation that the envelope p_{NL} varies slowly over the timescale of an optical cycle, so that $\frac{\partial^2 p_{NL}}{\partial t^2}, \omega_0\frac{\partial p_{NL}}{\partial t} << \omega_0^2 p_{NL}$, we can write:

$$\frac{\partial^2 P_{NL}}{\partial t^2}\cong-\omega_0^2 p_{NL}\;\exp\left[i\,\left(\omega_0 t-k_p z\right)\right] \tag{2.18}$$

and finally obtain the equation:

$$\frac{\partial A}{\partial z}+\frac{1}{v_{g0}}\frac{\partial A}{\partial t}-\frac{i}{2}k''_0\frac{\partial^2 A}{\partial t^2}=-i\,\frac{\mu_0\omega_0 c}{2n_0}\,p_{NL}\;\exp\left[-i\,\Delta k z\right] \tag{2.19}$$

where $\Delta k = k_p - k_0$ is the so-called "wave-vector mismatch" between the nonlinear polarisation and the field. This equation will be used in the next section to derive the coupled nonlinear equations for second-order parametric interaction.

2.3 Theory of Optical Parametric Amplification

Let us consider an optical field, consisting of the superposition of three waves, at frequencies ω_1, ω_2 and ω_3:

$$E\,(z,t)=\frac{1}{2}\left\{\begin{array}{l}A_1\,(z,t)\exp\left[i\,(\omega_1 t-k_1 z)\right]+A_2\,(z,t)\exp\left[i\,(\omega_2 t-k_2 z)\right]+\\ A_3\,(z,t)\exp\left[i\,(\omega_3 t-k_3 z)\right]+c.c.\end{array}\right\} \tag{2.20}$$

satisfying the condition $\omega_1+\omega_2=\omega_3$, impinging on a medium with a second order nonlinear response:

$$P_{NL}\,(z,t)=\varepsilon_0\chi^{(2)}E^2\,(z,t) \tag{2.21}$$

Such a situation is known as "nonlinear second-order parametric interaction" and corresponds to an exchange of energy between the three fields mediated by the second order nonlinearity. The nonlinear polarisation will contain three components at frequencies ω_1, ω_2 and ω_3, given by:

$$P_{1NL}(z,t) = \frac{\varepsilon_0 \chi^{(2)}}{2} A_2^* A_3 \exp\{i\,[\omega_1 t - (k_3 - k_2)\,z] + c.c.\} \tag{2.22a}$$

$$P_{2NL}(z,t) = \frac{\varepsilon_0 \chi^{(2)}}{2} A_1^* A_3 \exp\{i\,[\omega_2 t - (k_3 - k_1)\,z] + c.c.\} \tag{2.22b}$$

$$P_{3NL}(z,t) = \frac{\varepsilon_0 \chi^{(2)}}{2} A_1 A_2 \exp\{i\,[\omega_3 t - (k_1 + k_2)\,z] + c.c.\} \tag{2.22c}$$

Obviously there are other terms on P_{NL} at different frequencies, such as for example $2\omega_1$, $2\omega_2$, ω_1–ω_2 ... Here we consider only the terms at ω_1, ω_2 and ω_3 because we assume that only the interaction between these three fields is efficient, due to the phase-matching condition. We can then derive the following three equations for the fields at ω_1, ω_2 and ω_3:

$$\frac{\partial A_1}{\partial z} + \frac{1}{v_{g1}}\frac{\partial A_1}{\partial t} - \frac{i}{2}k''_1\frac{\partial^2 A_1}{\partial t^2} = -i\kappa_1 A_2^*\, A_3 \exp[-i\,\Delta k z] \tag{2.23a}$$

$$\frac{\partial A_2}{\partial z} + \frac{1}{v_{g2}}\frac{\partial A_2}{\partial t} - \frac{i}{2}k''_2\frac{\partial^2 A_2}{\partial t^2} = -i\kappa_2 A_1^*\, A_3 \exp[-i\,\Delta k z] \tag{2.23b}$$

$$\frac{\partial A_3}{\partial z} + \frac{1}{v_{g3}}\frac{\partial A_3}{\partial t} - \frac{i}{2}k''_3\frac{\partial^2 A_3}{\partial t^2} = -i\kappa_3 A_1\, A_2 \exp[i\,\Delta k z] \tag{2.23c}$$

where we have defined the nonlinear coupling coefficients: $\kappa_i = \dfrac{\omega_i \chi^{(2)}}{4cn_i}$ and the "wave-vector mismatch" as: $\Delta k = k_3 - k_1 - k_2$. The three equations are coupled nonlinear partial differential equations, are in general not amenable to an analytic solution and must be treated numerically. A first simplification, that captures the main physics of second order parametric interaction, consists in neglecting the GVD terms, i.e. putting $k''_i = 0$. This is justified by considering that the three interacting pulses are propagating with very different group velocities v_{gi}. Unless one considers ultrashort pulses, the effects of this group velocity mismatch (GVM) are much more relevant than those of GVD between the different frequency components of a single pulse. The coupled equations can be further simplified by moving to a frame of reference translating with the group velocity of the pump pulse $\tau = t - \dfrac{z}{v_{g3}}$, and become:

$$\frac{\partial A_1}{\partial z} + \delta_{13}\frac{\partial A_1}{\partial \tau} = -i\kappa_1 A_2^*\, A_3 \exp[-i\,\Delta k z] \tag{2.24a}$$

$$\frac{\partial A_2}{\partial z} + \delta_{23}\frac{\partial A_2}{\partial \tau} = -i\kappa_2 A_1^*\ A_3 \exp\left[-i\,\Delta k z\right] \tag{2.24b}$$

$$\frac{\partial A_3}{\partial z} = -i\kappa_3 A_1\ A_2 \exp\left[i\,\Delta k z\right] \tag{2.24c}$$

where $\delta_{i3} = \frac{1}{v_{gi}} - \frac{1}{v_{g3}}$ $i = 1, 2$ is the GVM between signal/idler and pump waves. These are nonlinear coupled partial differential equations that can be solved numerically. To get some physical insight, we can start by considering quasi-monochromatic waves, which allows us to set $\dfrac{\partial}{\partial \tau} = 0$. A further approximation can be made by assuming that the conversion efficiencies are so low that pump depletion can be neglected, i.e. $A_3 \cong A_{30} =$ constant. We thus obtain the nonlinear coupled equations for the signal and idler waves:

$$\frac{d\,A_1}{d\,z} = -i\kappa_1 A_3 A_2^*\ \exp\left[-i\,\Delta k z\right] \tag{2.25a}$$

$$\frac{d\,A_2}{d\,z} = -i\kappa_2 A_3 A_1^*\ \exp\left[-i\,\Delta k z\right] \tag{2.25b}$$

Equation (2.25a) can be easily rewritten as:

$$\frac{d^2 A_1}{d\,z^2} = -i\,\Delta k \frac{d\,A_1}{d\,z} + \Gamma^2 A_1 \tag{2.26}$$

where $\Gamma^2 = \dfrac{2{d_{eff}}^2 \omega_1 \omega_2}{c_0^3 \varepsilon_0 n_1 n_2 n_3} I_3$ and $I_3 = \frac{1}{2} n_3 c \varepsilon_0 |A_3|^2$ is the pump beam intensity. The nonlinear coefficient d_{eff} is proportional to the element of the $\chi^{(2)}$ tensor that keeps trace of the polarisation of the beams and their propagation directions within the nonlinear crystal lattice.

In the hypothesis of an initial signal field amplitude $A_1(0) = A_{10}$ (the "seed beam") and no initial idler ($A_2(0) = 0$), the solutions of Eqs. (2.25) are:

$$I_1(z) = I_{10}\left\{1 + \left[\frac{\Gamma}{g}\sinh\left(gz\right)\right]^2\right\} \tag{2.27a}$$

$$I_2(z) = I_{10}\frac{\omega_2}{\omega_1}\left[\frac{\Gamma}{g}\sinh\left(gz\right)\right]^2 \tag{2.27b}$$

where $g = \sqrt{\Gamma^2 - \left(\frac{\Delta k}{2}\right)^2}$. For the case of large gain ($gz >> 1$) Eqs. (2.27) further simplify to:

$$I_1(z) = \frac{I_{10}}{4}\left(\frac{\Gamma}{g}\right)^2 \exp\left(2gz\right) \tag{2.28a}$$

$$I_2(z) = \frac{\omega_2}{\omega_1} I_1(z) \tag{2.28b}$$

giving an exponential growth of both signal and idler intensities with crystal length, characteristic of an optical amplifier. It should also be noted, that, in the large gain limit, signal and idler intensities are related by energy conservation, since for each annihilated pump photon a signal and an idler photon are simultaneously generated.

The parametric gain for the signal beam, in the large gain limit, can be written as:

$$G = \frac{I_1(z)}{I_{s0}} = \frac{1}{4}\left(\frac{\Gamma}{g}\right)^2 \exp(2gz) \tag{2.29}$$

Let us now discuss the factors influencing this gain:

1. $G \propto \exp(g)$ exponentially depends on the parameter g, which is maximum when $\Delta k = 0$ (phase-matching condition). G rapidly decreases for non-zero values of Δk, suggesting that phase-matching is a key condition to be fulfilled in order to get significant amplification from the non-linear material.
2. $G \propto \exp(d_{eff})$ depends exponentially on the second order nonlinear optical coefficient of the crystal d_{eff}; one should therefore select the crystal with the largest nonlinear response. There are however other considerations leading to the choice of the crystal, such as phase matching range, dispersive properties, and optical damage threshold.
3. G scales as the exponential of the square root of the pump intensity. This indicates the suitability of ultrashort pulses for OPAs, due to their high peak powers. One should try to use the highest possible pump intensity before the onset of other nonlinear optical phenomena such as self-focusing, self-phase modulation and beam breakup. In order to be able to use high pump intensities, it is however important to have a spatially clean beam profile, without hot spots.
4. G scales as the exponential of the crystal length, as in an optical amplifier. With ultra-short light pulses, however, the optimum crystal length has to be chosen considering the durations and group velocities of the interacting pulses.
5. G scales as the exponential of the square root of the product of signal and idler frequencies. This seems to indicate an advantage to use higher pump frequencies. However we will see that with ultrashort pulses this advantage is often offset by the larger difference in group velocities of the interacting pulses.

The gain of an OPA is similar to that of a classical optical amplifier based on population inversion, but with some important differences;

1. an OPA does not have any energy storage capability, i.e. the gain is present only during the pump pulse;
2. the gain centre frequency is not fixed, but can be continuously adjusted by varying the phase-matching condition;
3. the gain bandwidth is not limited by the linewidth of the transition, as in an amplifier based on population inversion, but rather by the possibility of satisfying the phase-matching condition over a broad range of frequencies.

2.4 Parametric Amplification with Ultrashort Pulses

So far we have considered the theory of OPAs with monochromatic waves. When dealing with ultrashort pulses, one should in principle perform a full numerical solution of Eqs. (2.23). However, considerable physical insight can already be derived from the simpler Eqs. (2.24), showing that the efficiency of the process is governed by the GVM between the interacting pulses. In particular, GVM between the pump and the signal/idler pulses limits the interaction length over which parametric amplification takes place, while GVM between the signal and the idler beams limits the phase matching bandwidth [9]. Given a pump pulse with duration $\Delta\tau$, one can define a pulse splitting length L_{sp} as the propagation length after which the signal (or the idler) pulse temporally separates from the pump pulse in the absence of gain, which can be expressed as:

$$L_{spj3} = \frac{\Delta\tau}{|\delta_{j3}|} \quad j = 1, 2 \tag{2.30}$$

Note that the pulse splitting length becomes shorter for decreasing pulse duration and for increasing values of GVM, depending on the crystal type, pump wavelength and type of phase matching. There is a qualitatively significant difference between the cases in which δ_{13} and δ_{23} have the same or different signs. When $\delta_{13}\delta_{23} > 0$, both the signal and the idler pulses walk away from the pump in the same direction so that the gain rapidly decreases for propagation distances longer than the pulse splitting length and eventually saturates. On the other hand, when $\delta_{13}\delta_{23} < 0$, signal and idler pulses move in opposite direction with respect to the pump; in this way the signal and idler pulses tend to stay localized under the pump pulse and the gain grows exponentially even for crystal lengths well in excess of the pulse splitting length. This situation is illustrated in Fig. 2.2, showing simulations of the evolution of the temporal intensity profiles inside the gain medium, obtained by numerical solution of Eqs. (2.24).

Figure 2.2a shows a simulation for the case $\delta_{13}\delta_{23} > 0$; one can see that, for propagation lengths greater than the pulse splitting length, the parametric amplification process stops as the signal and idler pulses linearly walk away from the pump. Figure 2.2b shows a simulation for the case $\delta_{13}\delta_{23} < 0$. Here we see that the signal growth stays exponential for propagation distances well exceeding the pulse splitting length and that the signal pulse tends to stay localized under the pump. To understand this effect we can consider the situation in which the signal pulse has moved slightly to the left and the idler pulse to the right of the pump pulse. During the parametric amplification process, the signal pulse generates idler photons, which move to the right, i.e. towards the peak of the pump; in turn, the idler pulse generates signal photons which move to the left, again towards the peak of the pump. This concentration of photons under the peak of the pump explains the exponential gain growth overcoming GVM effects.

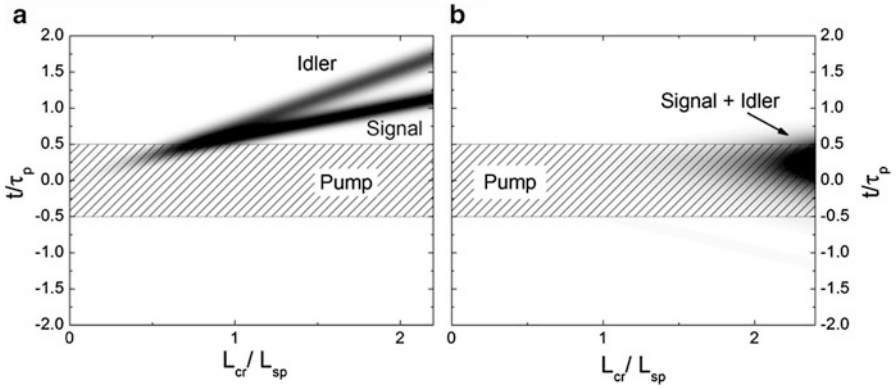

Fig. 2.2 Simulated signal intensity profiles of OPAs in a frame of reference moving with the pump pulse: (**a**) for the case $\delta_{13} > 0$, $\delta_{23} > 0$: signal and idler are slower than the pump and the effective crystal length is equal to the pulse splitting length between pump and signal, after which both pulses walk away from the pump; (**b**) for the case $\delta_{13} > 0$, $\delta_{23} < 0$: signal and idler walk in different directions with respect to the pump, as a result they stay trapped under the pump, increasing the interaction length

Let us now discuss which conditions determine the gain bandwidth of an OPA. Ideally one would like to have a broadband amplifier, i.e. an amplifier which, for a fixed pump frequency $\bar{\omega}_3$, provides a more or less constant gain over an as broad as possible range of signal frequencies. To this end, one needs to keep the phase mismatch Δk as small as possible over a large bandwidth. Practically, however, the phase-matching condition can be satisfied only for a given set of frequencies $(\bar{\omega}_1, \bar{\omega}_2, \bar{\omega}_3)$, such that:

$$\Delta k = k\,(\bar{\omega}_3) - k\,(\bar{\omega}_1) - k\,(\bar{\omega}_2) = 0 \tag{2.31}$$

If the pump frequency is fixed at $\bar{\omega}_3$ and the signal frequency changes to $\bar{\omega}_1 + \Delta\omega$, then by energy conservation the idler frequency changes to $\bar{\omega}_2 - \Delta\omega$. The ensuing wave vector mismatch becomes:

$$\Delta k = k\,(\bar{\omega}_3) - [k\,(\bar{\omega}_1) + \Delta k_1] - [k\,(\bar{\omega}_2) + \Delta k_2] = -\Delta k_1 - \Delta k_2 \tag{2.32}$$

which can be approximated to the first order as:

$$\Delta k = -\frac{\partial k_1}{\partial \omega_1}\Delta\omega + \frac{\partial k_2}{\partial \omega_2}\Delta\omega = \delta_{12}\Delta\omega \tag{2.33}$$

where $\delta_{12} = \dfrac{1}{v_{g2}} - \dfrac{1}{v_{g1}}$ is the GVM between signal and idler pulses. The full width at half maximum parametric gain bandwidth for a crystal of length L can then be calculated from Eq. (2.29), within the large gain and low pump-depletion approximations, as:

$$\Delta\omega = \frac{4\log(2)^{1/2}}{\pi}\left(\frac{\Gamma}{L}\right)^{1/2}\frac{1}{|\delta_{12}|} \tag{2.34}$$

Equation (2.34) shows that the gain bandwidth is inversely proportional to the GVM between signal and idler and has only a square root dependence on small-signal gain and crystal length. For the case when $v_{g1} = v_{g2}$ (group velocity matched OPA), Eq. (2.34) loses validity and (2.33) must be expanded to the second order in $\Delta\omega$, giving:

$$\Delta\omega = \frac{4\log(2)^{1/4}}{\pi}\left(\frac{\Gamma}{L}\right)^{1/4}\frac{1}{\left|k_1'' + k_2''\right|^{1/2}} \tag{2.35}$$

In this case the gain bandwidth is inversely proportional to the square root of the sum of the GVDs of signal and idler pulses. The conditions for achieving group-velocity matched OPAs will be discussed in Sect. 2.6.

2.5 Ultrafast OPA Architecture

A general scheme of an ultrafast OPA is presented in Fig. 2.3. The system is powered by energetic femtosecond pulses, such as those produced by an amplified Ti:sapphire laser at 800 nm or by an Ytterbium laser at 1 μm. A fraction of the beam is split and used to generate the seed beam. Then the pump beam (which may be optionally frequency doubled) and the seed, after their timing has been adjusted by a delay line, interact in a first amplification stage. It is possible to further amplify the signal in a second stage (power amplifier), using a previously split fraction of the pump beam. The two-stage approach has two advantages: (i) it allows one to compensate for the GVM arising between pump and signal pulses in the first stage; (ii) it enables one to adjust the pump intensity, and thus the parametric gain, separately in the two stages. In particular the power amplifier requires a much lower gain. At the OPA output, after the pump has been spectrally filtered, both signal and idler beams are available. In some cases, it may be necessary to use a pulse compressor to restore the transform-limited (TL) duration of the pulses.

The first stage of any OPA is the seed generator, i.e. a stage producing the initial photons at the signal wavelength. Since the seed beam is at a different wavelength with respect to the pump beam, a nonlinear process is required for its production. The two main techniques employed for seed generation are white-light continuum (WLC) generation and parametric superfluorescence. The WLC seed has the advantages of much higher stability and nearly diffraction-limited spatial beam quality, and is thus the most widely used.

As an example, we show in Fig. 2.4 a typical setup for a near-IR OPA [10]: it is pumped by an amplified Ti:sapphire laser generating 500-μJ, 50-fs pulses at 1 kHz repetition rate. A small fraction of the pump (≈2 μJ) is used to generate a WLC seed in a 2-mm-thick sapphire plate. 50 μJ are used to pump a pre-amplifier stage

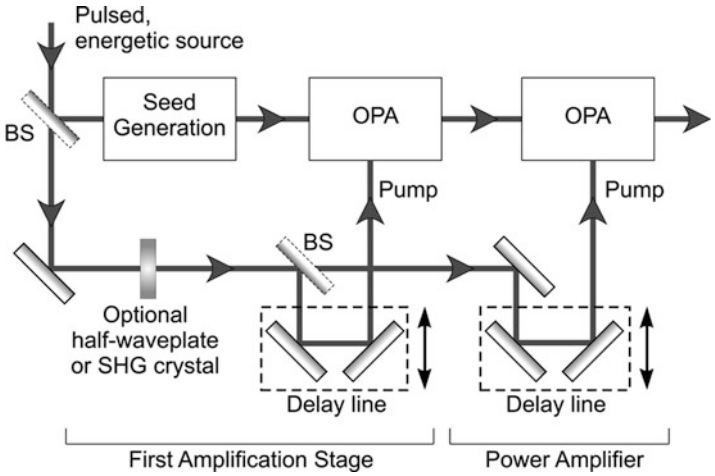

Fig. 2.3 Scheme of an ultrafast optical parametric amplifier. *BS* beam splitter, *OPA* optical parametric amplification stage

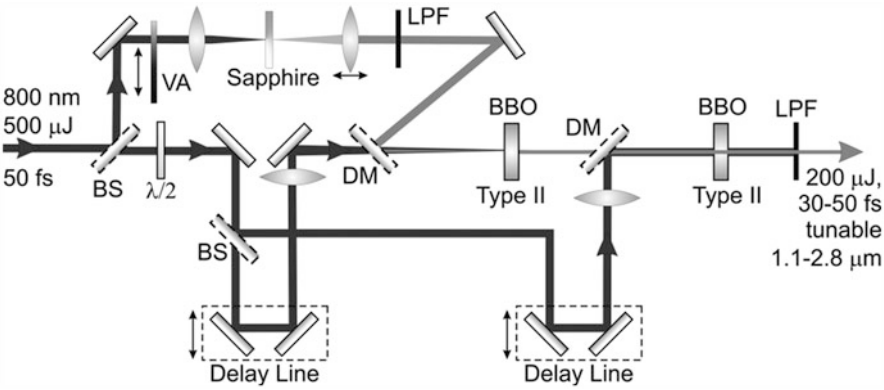

Fig. 2.4 Scheme of a near-IR OPA. *BS* beam splitter, *DM* dichroic mirror, *LPF* long-pass filter, *VA* variable attenuator

consisting of a 3-mm-thick β-barium borate (BBO) crystal cut for type II phase matching ($\theta = 26°$, $\varphi = 0°$). Wavelength tuning is achieved by tilting the crystal, thus changing the phase-matching condition. Typical signal energies after the pre-amplifier are up to 6 μJ. The power amplifier stage consists of an identical BBO crystal pumped by 450 μJ; in this case amplified pulse energies up to 200 μJ are generated. The signal beam is tuneable from 1.1 to 1.6 μm and the idler up to 2.8 μm, limited by absorption in the BBO crystal; pulsewidth ranges from 30 to 50 fs according to wavelength.

2.6 Ultra-Broadband OPAs

Equation (2.34) makes it clear that, in order to obtain broad phase matching bandwidths, one must achieve, for a given signal frequency $\bar{\omega}_1$, $\delta_{12} = 0$, i.e. group velocity matching between signal and idler pulses. It will then become possible to amplify a broad bandwidth centred around $\bar{\omega}_1$. We will show in the following that, by using suitable non-linear crystals, pump frequencies and phase-matching configurations $\bar{\omega}_1$ can be varied over a very broad range, spanning from the visible to the mid-infrared, enabling the generation of widely tuneable few-optical-cycle light pulses from OPAs.

In an OPA using a collinear interaction geometry, the propagation direction inside the nonlinear crystal is selected to satisfy the phase-matching condition ($\Delta k = 0$) for a given signal wavelength. In this configuration the signal and idler group velocities are in general not matched. Group velocity matching can be obtained in a *type I* (or *type 0* in a periodically poled crystal) *degenerate configuration*, in which signal and idler have the same frequency ($\omega_1 = \omega_2 = \omega_3/2$) and the same polarisation.

If the signal wavelength is tuned away from degeneracy, then the $\delta_{12} = 0$ condition is generally not fulfilled in a collinear configuration, leading to narrow phase-matching bandwidths. An additional degree of freedom can be introduced using a non-collinear geometry [11], in which pump and signal wave-vectors form an angle α (independent of signal wavelength) and the idler is emitted at an angle Ω with respect to the signal. In this case the phase matching condition is a vector equation, $\boldsymbol{k_3} = \boldsymbol{k_1} + \boldsymbol{k_2}$ that, when projected on directions parallel and perpendicular to the signal wave-vector, becomes:

$$k_3 \cos\alpha = k_1 + k_2 \cos\Omega \tag{2.36a}$$

$$k_3 \sin\alpha = k_2 \sin\Omega \tag{2.36b}$$

Note that the angle Ω is not fixed, but it depends on the idler frequency according to Eq. (2.36b). If the signal frequency increases by $\Delta\omega$, the idler frequency decreases by $\Delta\omega$ and the wave-vector mismatches along the two directions parallel and perpendicular to the signal wavevector can be approximated, to the first order, as:

$$\Delta k_{par} \cong -\frac{\partial k_1}{\partial \omega_1}\Delta\omega + \frac{\partial k_2}{\partial \omega_2}\cos\Omega\,\Delta\omega - k_2 \sin\Omega \frac{\partial \Omega}{\partial \omega_2}\Delta\omega \tag{2.37a}$$

$$\Delta k_{perp} \cong \frac{\partial k_2}{\partial \omega_2}\sin\Omega\,\Delta\omega + k_2 \cos\Omega \frac{\partial \Omega}{\partial \omega_2}\Delta\omega \tag{2.37b}$$

To achieve broadband phase matching, both Δk_{par} and Δk_{perp} must vanish. Upon multiplying (2.37a) by cosΩ and (2.37b) by sinΩ and adding the results, we get

$$\frac{\partial k_2}{\partial \omega_2} - \cos\Omega \frac{\partial k_1}{\partial \omega_1} = 0 \tag{2.38}$$

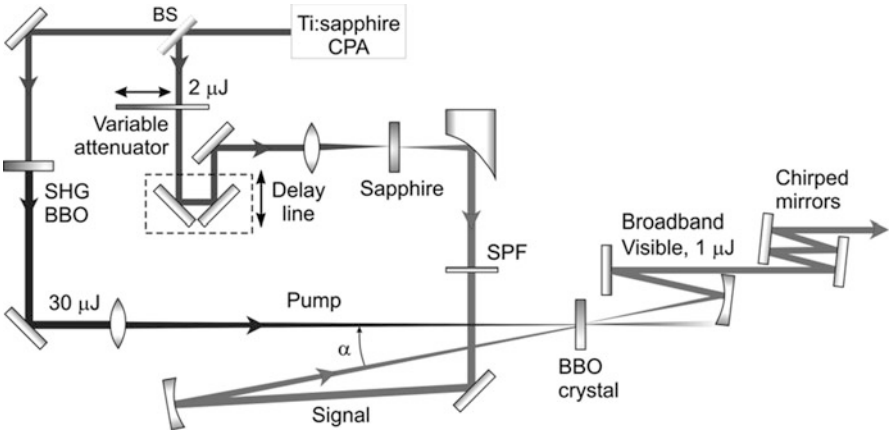

Fig. 2.5 Scheme of a BBO based NOPA pumped at 400 nm. *BS* beam splitter, *SPF* shortpass filter

which is equivalent to:

$$v_{g1} = v_{g2} \cos \Omega \tag{2.39}$$

Equation (2.39) lends itself to a very simple geometrical interpretation [12]: in a non-collinear configuration, broadband phase matching can be achieved for a signal-idler angle Ω such that the signal group velocity equals the projection of the idler group velocity along the signal direction. The so-called non-collinear OPA (NOPA), is a widely used device for the generation of few-optical-cycle pulses in the visible range [13–18]. In a practical situation the pump-signal angle α is determined by the propagation direction of the seed beam, while the signal-idler angle Ω adjusts itself, according to (2.36b), to satisfy the phase-matching condition. For this reason, the idler is emitted at a different angle for each wavelength, i.e., it is angularly dispersed and not easily usable.

In the following we will describe a typical visible NOPA design [19], the schematic of which is shown in Fig. 2.5. The system is pumped by an amplified Ti:sapphire laser generating 150-fs, 800-nm pulses at 1 kHz with energy up to 500 μJ. The energy is sufficient for simultaneously pumping several independent NOPAs. A fraction of the beam is used to generate the pump pulses at 400 nm by second-harmonic generation in a 1-mm-thick BBO crystal; pulse energies up to 30 μJ are used to pump the first stage. Another small fraction of the beam, with energy of approximately 2 μJ, is focused into a 1-mm-thick sapphire plate to generate the WLC seed; by carefully controlling the energy incident on the plate (using a variable-optical-density attenuator) and the position of the plate around the focus, a highly stable single-filament WLC is generated. The chirp of the visible portion of the white light is small and fairly linear with frequency. To avoid the introduction of additional chirp, only reflective optics are employed to guide the WLC to the amplification stage. Parametric gain is achieved in a 1-mm-thick BBO

crystal, cut for type I phase matching ($\theta = 32°$), using a single-pass configuration to increase the gain bandwidth. The chosen crystal length is close to the pulse-splitting length L_{sp13} for signal and pump in the visible wavelength range. To minimize the effects of self-focusing, the BBO crystal is beyond the focus of the pump beam. The WLC seed is imaged by a spherical mirror in the BBO crystal, with a 100-μm spot size matching that of the pump beam. A thin short-pass filter removes the strong residual 800-nm component from the WLC, preventing its parasitic amplification.

When the BBO crystal is illuminated by the pump pulse and aligned perpendicularly to the pump beam, it emits a strong off-axis parametric superfluorescence in the visible in the form of a cone with apex angle of $\approx 6.2°$ (corresponding to an angle of 3.82° inside the crystal); this is the direction for which the group velocities of signal and idler are matched and therefore the gain bandwidth is maximized. The visible cone gives a visual aid to the identification of the optimum condition for broadband generation, which is found when the pump-signal angle matches the cone apex angle. In this condition, for optimum pump–seed delay, an ultrabroad gain bandwidth that extends over most of the visible (500–750 nm) is observed. The amplified pulses from a single stage have energy of approximately 2 μJ; much higher energies, up to ≈300 μJ [20], can be extracted by a second amplification stage. After the gain stage the amplified pulses are collimated by a spherical mirror and sent to the compressor.

Several compressor schemes have been implemented for the visible NOPA. Simple prism pairs can correct the second but not third-order dispersion and thus can only compress the pulses down to 10–15 fs; sub-10-fs pulses can be achieved by using either prism-grating [17] or prism-chirped mirrors combinations, as well as adaptive compressors based on deformable mirrors [20–22]. It is also possible to use exclusively chirped mirrors [19, 23], greatly simplifying the system design, allowing for compactness, insensitivity to misalignment and high day-to-day reproducibility, which are of great importance in practical applications.

2.7 Carrier-Envelope Phase Stabilization in an OPA

The previous paragraphs illustrated ultra-broadband OPA configurations capable of producing widely tuneable few-optical-cycle pulses. Here we will show how these schemes can be extended to the synthesis of pulses with controlled carrier-envelope phase (CEP), i.e. with an electric field profile reproducible from shot to shot. Mathematically, the electric field of an ultrashort pulse can be written as:

$$E(t) = A(t)\cos(\omega_c t + \phi) \tag{2.40}$$

where $A(t)$ is the pulse envelope with its maximum at $t = 0$, ω_c is the carrier frequency and ϕ is the CEP. If $\phi = 0$, a maximum of the electric field corresponds to the peak of the pulse envelope (cosine pulse), while if $\phi = \pi/2$ the electric field at the peak of the pulse envelope is zero (sine pulse). Control of the CEP

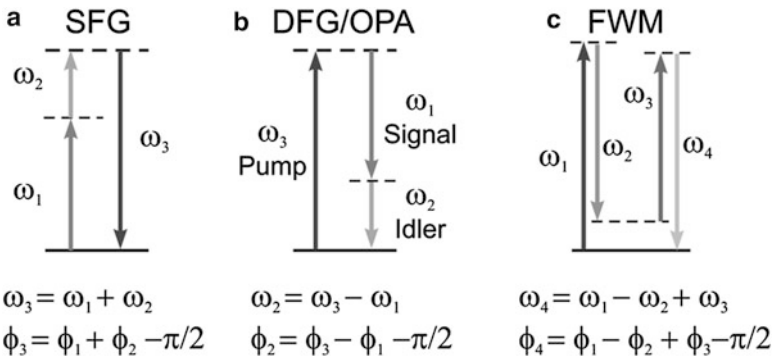

Fig. 2.6 Frequency and phase summation rules for (**a**) sum-frequency generation (SFG), (**b**) difference-frequency generation (*DFG*), equivalent to the generation of the idler wave in an OPA, and (**c**) a four-wave mixing process (*FWM*)

becomes important for few-optical-cycle light pulses and for extreme nonlinear optics experiments, which are sensitive to the electric field rather than the intensity of the pulse.

Typical femtosecond laser sources generate a pulse train in which the CEP is not stabilized, so that ϕ varies randomly from shot to shot. CEP can be stabilized using either active or passive methods. Active control starts by measuring the pulse-to-pulse CEP slip $\Delta\phi$ in a mode-locked oscillator and stabilizing it by active electronic feedback [24]; by picking pulses at a fraction of the laser repetition rate, it is possible to obtain a train of pulses with a constant absolute phase, which can be further amplified. A completely different approach is passive CEP stabilization, which exploits nonlinear optical effects to generate a pulse train with stable CEP [25].

To understand passive CEP stabilization, let us review the effect of different nonlinear processes on the CEPs of the interacting pulses. For the second-order process of Sum-Frequency Generation (SFG), in which two pulses at frequencies ω_1 and ω_2, with CEPs ϕ_1 and ϕ_2, generate the sum frequency $\omega_3 = \omega_1 + \omega_2$, the CEP of the resulting pulse is $\phi_3 = \phi_1 + \phi_2 - \pi/2$ (Fig. 2.6a). For the particular case of second harmonic generation (SHG) starting from a pulse with frequency ω_0 and CEP ϕ, one obtains a pulse with frequency $\omega_{SH} = 2\omega_0$ and CEP $\phi_{SH} = 2\phi - \pi/2$. In the second-order process of Difference-Frequency Generation (DFG) between two pulses at frequencies ω_1 and ω_3, with CEPs ϕ_1 and ϕ_3, the resulting difference-frequency pulse has frequency $\omega_1 = \omega_3 - \omega_2$ and CEP $\phi_1 = \phi_3 - \phi_2 - \pi/2$ (Fig. 2.6b). In the third order non-linear process of Four-Wave Mixing (FWM), four waves at frequencies ω_1, ω_2, ω_3 and ω_4, with $\omega_4 = \omega_1 - \omega_2 + \omega_3$, are coupled in a $\chi^{(3)}$ nonlinear medium. In this case, the CEPs of the waves are linked by the relationship: $\phi_4 = \phi_1 - \phi_2 + \phi_3 - \pi/2$ (Fig. 2.6c). Self-Phase Modulation (SPM), i.e. spectral broadening due to the instantaneous intensity-dependent variations of index of refraction in a Kerr medium, can be regarded as a special case of FWM, in which a new frequency ω_{SPM} is generated starting from three frequencies ω_1, ω_2 and ω_3, all belonging to the pulse spectrum, according to the FWM process:

$\omega_{SPM} = \omega_1 + \omega_2 - \omega_3$. These new frequencies in turn contribute to subsequent FWM processes, causing a progressive broadening of the pulse spectrum as it propagates through the nonlinear medium. If we now consider that the mixing pulses share the same CEP $\phi_1 = \phi_2 = \phi_3 = \phi$, then the SPM pulse will have the CEP $\phi_{SPM} = \phi_1 - \phi_2 + \phi_3 - \pi/2 = \phi - \pi/2$. Thus the newly added frequency components of the broadened SPM spectrum inherit the original value of the CEP of the driving pulse. The SPM/FWM process is the dominant nonlinear interaction behind WLC generation.

Having clarified the effects of nonlinear optical processes on the CEPs of the interacting pulses, we are now in a position to understand the passive CEP stabilization method. If a DFG process $\omega_{DF} = \omega_2 - \omega_1$ occurs between two pulses with the same shot-to-shot CEP fluctuations ($\phi_1 = \phi + c_1$, $\phi_2 = \phi + c_2$), then $\phi_{DF} = c_2 - c_1 - \pi/2 = \text{const.}$, i.e., the fluctuations of ϕ are automatically cancelled [25]. Passive CEP stabilization has some clear advantages with respect to the active one: (i) it is an all-optical technique and does not require any electronic feedback circuits; (ii) it directly produces a train of CEP-stable pulses, avoiding the need to pick pulses.

Let us now discuss how CEP stable pulses can be generated from an OPA. We start by recalling that the idler pulse is generated through a DFG process between pump and signal, so that its CEP, according to the previous discussion, is given by $\phi_2 = \phi_3 - \phi_1 - \pi/2$. Let us now consider an OPA that is pumped by pulses at the fundamental frequency (FF) ω_0, with CEP $\phi_3 = \phi$ which is generally fluctuating from shot to shot. If the seed pulse is produced via WLC generation starting from the FF pulse, then its CEP is linked to that of the pump by $\phi_1 = \phi - \pi/2$ (see Fig. 2.7c); in this case the idler has CEP $\phi_2 = 0$, which is stable from shot to shot (Fig. 2.7b). When the OPA is pumped by the second harmonic (SH) of the driving pulse, then $\phi_3 = 2\phi - \pi/2$; if the WLC seed is generated from the SH of the driver, then $\phi_1 = 2\phi - \pi$ and $\phi_2 = 0$ (Fig. 2.7). We can thus conclude that an OPA generates a CEP stable idler when the seed is generated with the same pulse used as the pump, either the FF or the SH of the driving laser.

If, on the other hand, the OPA is pumped by the SH but the seed is generated from the FF, we have $\phi_3 = 2\phi - \pi/2$ and $\phi_1 = \phi - \pi/2$. In this case, we obtain $\phi_2 = \phi - \pi/2$, so that the idler is not CEP stabilized, but rather reproduces, from shot to shot, the CEP fluctuations of the driving pulse [26].

2.8 Optical Parametric Chirped Pulse Amplification

In a broadband OPA both the pump and the seed are femtosecond pulses, typically generated by a Ti:sapphire system. It is generally difficult and expensive to scale the energy of femtosecond pump lasers; on the other hand, it is easier to generate energetic picosecond pulses (5–50 ps duration) exploiting well-established gain media such as Nd: or Yb:doped crystals. With a long pump pulse, in order to achieve efficient energy extraction, it is necessary to temporally overlap the seed pulse with the pump by first stretching the seed pulse and then, after the amplification

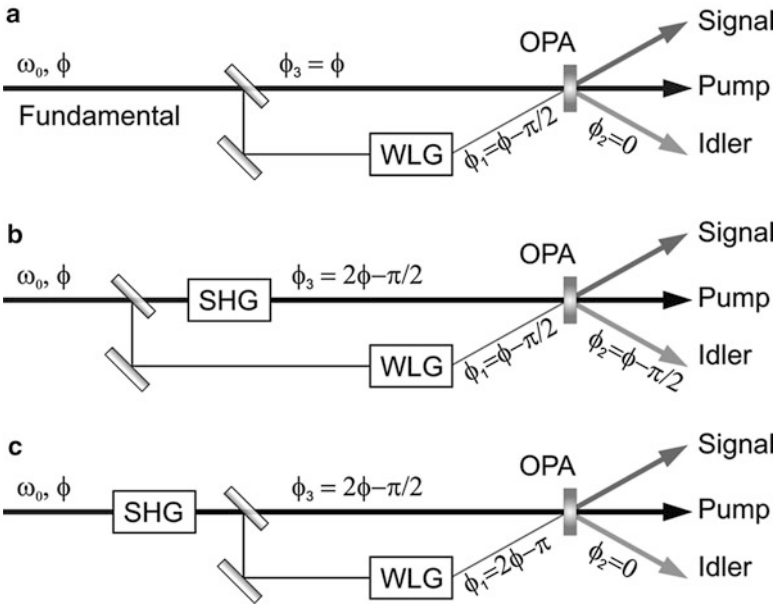

Fig. 2.7 Schematics of three OPA configurations. For clarity, the seed and the pump beams are shown to intersect non-collinearly in the crystal. However, the conclusions are also valid for the collinear beam arrangement

step, recompressing it back to nearly TL durations. This scheme, which is very similar to the Chirped Pulse Amplification (CPA) [27] occurring in a real gain medium, is known as OPCPA [28, 29] and is considered as the most promising route for energy scaling of few-optical-cycle pulses [30]. The key technical hurdle in OPCPAs is the synchronization of the pump and seed pulses; it can be achieved either electronically, using suitable circuitry, or optically, by using a part of the seed pulse spectrum to injection seed the pump laser. The optical approach allows a much lower pump-seed timing jitter but it is more challenging, since pump and seed are at different frequencies.

The OPA/OPCPA approaches offer some distinct advantages with respect to CPA for the generation of high peak power few-optical-cycle pulses:

1. the OPA/OPCPA has the capability of providing a high gain in a relatively short path, allowing a compact, tabletop amplifier setup, minimizing the linear and nonlinear phase distortions and ensuring an excellent temporal and spatial quality of the pulses.
2. with suitable selection of the phase-matching conditions (see Sect. 2.6), the OPA process can provide gain bandwidths well in excess of those achievable with conventional amplifiers and can sustain pulse spectra corresponding to a TL duration of just a few cycles of the carrier frequency.

3. in an OPCPA, amplification occurs only during the pump pulse, so that amplified spontaneous emission and the consequent pre-pulse pedestal are greatly reduced.
4. since the OPA/OPCPA is an instantaneous process of energy exchange between the interacting beams, no fraction of the pump photon energy is deposited in the medium; thus, if parasitic pump absorption can be neglected, thermal loading effects are absent, greatly reducing spatial aberrations of the beams. This allows much higher repetition rates to be achieved while avoiding the heat removal problems that limit the frequency scaling of CPA systems.

In addition to these clear advantages, the OPA/OPCPA concept also has some drawbacks:

1. an OPA/OPCPA requires pump pulses with short duration (hundreds of femtoseconds to tens of picoseconds), which are technologically challenging to generate, especially at high energy and/or high repetition rate; on the other hand the CPA, thanks to energy storage in the excited state, can use much longer nanosecond pump pulses (or even continuous wave pumping for materials with long excited state lifetime like Yb-doped crystals);
2. an OPA/OPCPA is very sensitive to the spatial and temporal quality of the pump, again putting a severe technological constraint on the pump laser.

2.9 Conclusions

This chapter has provided a brief review of the principles of ultrashort pulse OPAs, focusing in particular on the generation of few-optical-cycle pulses. After discussing the propagation of an ultrashort pulse in a nonlinear medium and reviewing the theory of parametric amplification, we considered the typical architecture of an ultrafast OPA. This chapter went on to discuss non-collinear OPAs, which are widely used for the generation of few-optical-cycle pulses in the visible range and capable of producing pulses with energies of $2\,\mu$J, which can be further amplified to 300 μJ. These schemes can be extended for the synthesis of pulses with controlled carrier-envelope phase. Indeed, the last section of this chapter introduces the concept of optical parametric chirped pulse amplification, which is considered the most promising approach for energy scaling of few-optical-cycle pulses.

References

1. A.H. Zewail, Femtochemistry: atomic-scale dynamics of the chemical bond. J. Phys. Chem. A **104**, 5660–5694 (2000)
2. C. Manzoni, D. Polli, G. Cerullo, Two-color pump-probe system broadly tunable over the visible and the near infrared with sub-30 fs temporal resolution. Rev. Sci. Instrum. **77**, 023103–023112 (2006)
3. F. Krausz, M. Ivanov, Attosecond physics. Rev. Mod. Phys. **81**, 163–234 (2009)

4. F.X. Kärtner, *Few-Cycle Laser Pulse Generation and Its Applications* (Springer, Berlin, 2004)
5. J.A. Giordamaine, R.C. Miller, Tunable coherent parametric oscillation in $LiNbO_3$ at optical frequencies. Phys. Rev. Lett. **14**, 973–976 (1965)
6. R.A. Baumgartner, R.L. Byer, Optical parametric amplification. IEEE J. Quantum Electron. **15**, 432–444 (1979)
7. Y.R. Shen, *The Principles of Nonlinear Optics* (Wiley, New York, 1984)
8. R. Boyd, *Nonlinear Optics* (Academic, New York, 1992)
9. G. Cerullo, S. De Silvestri, Ultrafast optical parametric amplifiers. Rev. Sci. Instrum. **74**, 1–18 (2003)
10. D. Brida, G. Cirmi, C. Manzoni, S. Bonora, P. Villoresi, S. De Silvestri, G. Cerullo, Sub-two-cycle light pulses at 1.6 μm from an optical parametric amplifier. Opt. Lett. **33**, 741–743 (2008)
11. G.M. Gale, M. Cavallari, T.J. Driscoll, F. Hache, Sub-20-fs tunable pulses in the visible from an 82-MHz optical parametric oscillator. Opt. Lett. **20**, 1562–1564 (1995)
12. E. Riedle, M. Beutter, S. Lochbrunner, J. Pielm, S. Schenkl, S. Spörlein, W. Zinth, Generation of 10 to 50 fs pulses tunable through all of the visible and the NIR. Appl. Phys. B **71**, 457–465 (2000)
13. T. Wilhelm, J. Piel, E. Riedle, Sub-20-fs pulses tunable across the visible from a blue-pumped single-pass noncollinear parametric converter. Opt. Lett. **22**, 1494–1497 (1997)
14. G. Cerullo, M. Nisoli, S. De Silvestri, Generation of 11 fs pulses tunable across the visible by optical parametric amplification. Appl. Phys. Lett. **71**, 3616–3618 (1997)
15. A. Shirakawa, T. Kobayashi, Noncollinearly phase-matched femtosecond optical parametric amplification with a 2000 cm^{-1} bandwidth. Appl. Phys. Lett. **72**, 147–149 (1998)
16. G. Cerullo, M. Nisoli, S. Stagira, S. De Silvestri, Sub-8-fs pulses from an ultrabroadband optical parametric amplifier in the visible. Opt. Lett. **23**, 1283–1285 (1998)
17. A. Shirakawa, I. Sakane, T. Kobayashi, Pulse-front-matched optical parametric amplification for sub-10-fs pulse generation tunable in the visible and near infrared. Opt. Lett. **23**, 1292–1294 (1998)
18. A. Shirakawa, I. Sakane, M. Takasaka, T. Kobayashi, Sub-5-fs visible pulse generation by pulse-front-matched noncollinear optical parametric amplification. Appl. Phys. Lett. **74**, 2668–2670 (1999)
19. M. Zavelani-Rossi, G. Cerullo, S. De Silvestri, L. Gallmann, N. Matuschek, G. Steinmeyer, U. Keller, G. Angelow, V. Scheuer, T. Tschudi, Pulse compression over a 170-THz bandwidth in the visible by use of only chirped mirrors. Opt. Lett. **26**, 1155–1157 (2001)
20. P. Tzankov, J. Zheng, M. Mero, D. Polli, C. Manzoni, G. Cerullo, 300 μJ noncollinear optical parametric amplifier in the visible at 1 kHz repetition rate. Opt. Lett. **31**, 3629–3631 (2006)
21. M.R. Armstrong, P. Plachta, E.A. Ponomarev, R.J.D. Miller, Versatile 7-fs optical parametric pulse generation and compression by use of adaptive optics. Opt. Lett. **26**, 1152–1154 (2001)
22. A. Baltuška, T. Fuji, T. Kobayashi, Visible pulse compression to 4 fs by optical parametric amplification and programmable dispersion control. Opt. Lett. **27**, 306–308 (2002)
23. P. Baum, M. Breuer, E. Riedle, G. Steinmeyer, Brewster-angled chirped mirrors for broadband pulse compression without dispersion oscillations. Opt. Lett. **31**, 2220–2222 (2006)
24. D.J. Jones, S.A. Diddams, J.K. Ranka, A. Stentz, R.S. Windeler, J.L. Hall, S.T. Cundiff, Carrier-envelope phase control of femtosecond mode-locked lasers and direct optical frequency synthesis. Science **288**, 635–639 (2000)
25. A. Baltuška, T. Fuji, T. Kobayashi, Controlling the carrier-envelope phase of ultrashort light pulses with optical parametric amplifiers. Phys. Rev. Lett. **88**, 133901–133905 (2002)
26. A. Baltuška, T. Fuji, T. Kobayashi, Self-referencing of the carrier-envelope slip in a 6-fs visible parametric amplifier. Opt. Lett. **27**, 1241–1243 (2002)
27. S. Backus, C.G. Durfee, M.M. Murnane, H.C. Kapteyn, High power ultrafast lasers. Rev. Sci. Instrum. **69**, 1207–1223 (1998)
28. A. Dubietis, G. Jonušauskas, A. Piskarskas, Powerful femtosecond pulse generation by chirped and stretched pulse parametric amplification in BBO crystal. Opt. Commun. **88**, 437–440 (1992)

29. A. Dubietis, R. Butkus, A.P. Piskarskas, Trends in chirped pulse optical parametric amplification. IEEE J. Sel. Top. Quantum Electron. **12**, 163–172 (2006)
30. D. Herrmann, L. Veisz, R. Tautz, F. Tavella, K. Schmid, V. Pervak, F. Krausz, Generation of sub-three-cycle, 16 TW light pulses by using noncollinear optical parametric chirped-pulse amplification. Opt. Lett. **34**, 2459–2461 (2009)

http://www.springer.com/978-3-319-00017-6

Ultrafast Nonlinear Optics
Thomson, R.; Leburn, C.; Reid, D. (Eds.)
2013, XVI, 377 p.,
ISBN: 978-3-319-00017-6